

Note

Nonphysical Self Forces in Some Electromagnetic Plasma-Simulation Algorithms

This note describes a simple algorithm for removing nonphysical self forces from two popular electromagnetic plasma simulation models. This algorithm also has two additional features; it is expected to reduce short-wavelength noise and unwanted numerical fluctuations and permits faster integration of the particle orbit equations by roughly a factor of two. It is currently being included in the CLYRAD code [1, 2].

There are three major numerical models in which electromagnetic radiation fields are self-consistently coupled to the Lorentz–Newton equations for the charged-particle motion. The first of these, proposed by Buneman [3], includes an explicit leapfrog algorithm for solving the Maxwell equations and a special charge-current algorithm, based on the NGP (Nearest Grid Point) particle interpolation, which ensures that the continuity equation for charge and current is automatically satisfied at each timestep in finite-difference form. The second of these three algorithms [1] uses essentially the same field treatment but has a more flexible treatment of current accumulation in which, however, a Poisson equation must be solved. The third algorithm [1] differs from the first two in the treatment of the electromagnetic fields. Rather than a finite difference approximation to the Maxwell equations, the algorithm solves the Fourier transform of the equations in \mathbf{k} -space. This third algorithm has not been implemented in multidimensions, but a fore-runner method in one dimension was devised by Langdon and Dawson [4].

Many variations of the first two algorithms are possible and several have been coded and used [5, 6]. Two of these are the Morse–Nielson algorithms *A* and *B*. Their algorithm *A* is an important generalization of Buneman’s algorithm to the PIC (particle-in-cell) linear interpolation [8, 9]. This algorithm also satisfies Poisson’s equation automatically at every timestep. The Morse–Nielson algorithm *B*, as pointed out by Langdon [7], is essentially equivalent to the Boris algorithm. Thus, our comments apply to the Boris algorithm used in CYLRAD, to both Morse–Nielson algorithms and to the Sinz [5] algorithm.

These electromagnetic algorithms treat particles moving on staggered, interlaced grids of variables as shown in Fig. 1 for two dimensions. Each field variable is so positioned that the time-dependent Maxwell equations reduce to an extremely simple, finite-difference form for advancing \mathbf{E} and \mathbf{B} which is reversible and

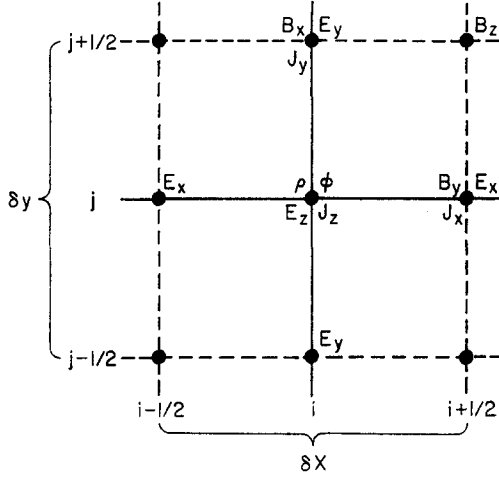


FIG. 1. The staggered-interlaced grids of a 2D electromagnetic simulation code. In three dimensions the E_x , J_x , B_x , and B_y grids are all displaced half a cell, $\delta z/2$ out of the plane of the figure.

second-order accurate. The generalization of this 2D field-variable arrangement to 3D is straightforward and the specialization to 1D is trivial. As can be seen, the finite-difference form of the divergence equation which should be satisfied at each cycle is

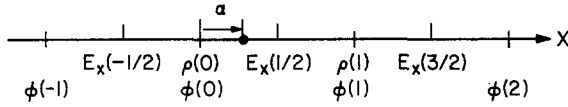
$$\frac{(E_x(i + \frac{1}{2}, j) - E_x(i - \frac{1}{2}, j))}{\delta x} + \frac{(E_y(i, j + \frac{1}{2}) - E_y(i, j - \frac{1}{2}))}{\delta y} = 4\pi\rho(i, j). \quad (1)$$

The electrostatic fields which result from placing a particle at rest on the (i, j) grid point are different from those found in an electrostatic code because the x and y electric field grids are displaced, as seen in Fig. 1, by $\delta x/2$ and $\delta y/2$, respectively, from the positions they would occupy in a standard electrostatic code [8, 9]. To simplify the analysis, the electrostatic and the electromagnetic grids are compared in Fig. 2 for a 1D case where a test particle of unit charge is at position α off a grid point ($0 < \alpha < \delta x/2 = 1/2$).

Consider first the electromagnetic grid as used in current simulation codes (Fig. 2). The linearly interpolated charge density at grid points 0 and 1 are $\rho(0) = 1 - \alpha$ and $\rho(1) = \alpha$. If $\pm E_{1/2}$, $\pm E_{3/2}$ are defined to be the electric field at $x = \pm 1/2$ and $x = \pm 3/2$, respectively, due to a unit charge at $x = 0$, then summing the contributions from the two grid points one gets

$$\begin{aligned} E_x(-1/2) &= -(1 - \alpha) E_{1/2} - \alpha E_{3/2}, \\ E_x(1/2) &= (1 - \alpha) E_{1/2} - \alpha E_{1/2}, \\ E_x(3/2) &= (1 - \alpha) E_{3/2} + \alpha E_{1/2}. \end{aligned} \quad (2)$$

ELECTROMAGNETIC GRID:



ELECTROSTATIC GRID:

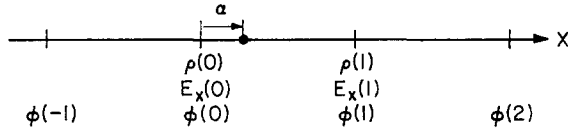


FIG. 2. Comparison of grids for standard electromagnetic and standard electrostatic algorithms in 1D. The staggered electromagnetic grid has electric fields defined at points half a cell removed from the points of charge-density definition.

Since the particle lies between $E_x(1/2)$ and $E_x(-1/2)$, the linearly interpolated x electric field, as would be found by an electromagnetic simulation code, is

$$\begin{aligned}
 E_x(\alpha) &= (1/2 + \alpha) E_x(1/2) + (1/2 - \alpha) E_x(-1/2) \\
 &= 2\alpha(1 - 2\alpha)[E_{1/2} - (E_{1/2} + E_{3/2})/4] \neq 0.
 \end{aligned}
 \tag{3}$$

Equation (3) shows that the self electrostatic field of a single simulation particle is nonzero. Thus, all sorts of spurious effects can result. Figure 3, shows a 1D plot of the equivalent potential a particle would see due to its self-force. We have carried out tests on an electromagnetic code, and the oscillations of a particle in this self field have been observed. The preceding analysis has been generalized to electrostatic and magnetostatic self-forces in two and three dimensions. In every case the results are the same; spurious electrostatic and magnetostatic forces are found when the charges do not exactly lie on grid lines. We know that there are no self forces

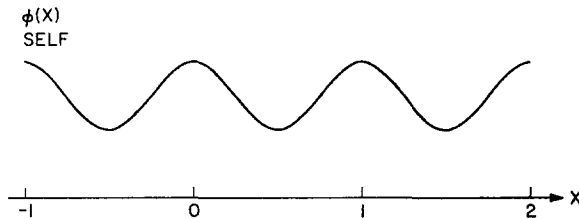


FIG. 3. The electrostatic self potential of a particle on a staggered 1D electromagnetic grid.

in the usual electrostatic codes [8, 9] and the electrostatic-code field in Fig. 2 are clearly closely related to the electromagnetic-code fields. Therefore, it should be a simple matter to eliminate the electrostatic self-forces from the electromagnetic-code. From Fig. 2 we have

$$E_x(1/2) = [\Phi(1) - \Phi(0)]/\delta x \quad (4)$$

and

$$E_x(0) = [\Phi(1) - \Phi(-1)]/\delta x. \quad (5)$$

The fields are, therefore, related by

$$E_x(0) = 1/2[E_x(1/2) + E_x(-1/2)]. \quad (6)$$

If we linearly interpolate to the particle position using the averaged fields of Eqs. (6) and (2), we get

$$\begin{aligned} E_x(\alpha) &= (1 - \alpha) E_x(0) + \alpha E_x(1) \\ &= 0. \end{aligned} \quad (7)$$

This is the desired result of zero self force. When generalized to two and three dimensions, the electrostatic and magnetostatic self forces are found to be zero. Furthermore, since the argument is basically one of symmetry rather than being based on any particular force law, the determination of $\Phi(i)$ from $\rho(i)$ admits all finite-sized particle algorithms as well as the 3, 5, and 7 point Poisson operators found in one, two, and three dimensions.

The averaging algorithm developed here for fully electromagnetic simulations in two dimensions is an obvious extension of Eq. (6) to the field-variable layout shown in Fig. 1. The three components of particle current density $J_x^p(i, j)$, $J_y^p(i, j)$ and $J_z^p(i, j)$ are all found by linear interpolation onto the (i, j) grid, exactly as $\rho(i, j)$. The current densities for use on the interlaced field grids are then computed as follows:

$$\begin{aligned} J_x(i + 1/2, j) &\equiv 1/2[J_x^p(i, j) + J_x^p(i + 1, j)], \\ J_y(i, j + 1/2) &\equiv 1/2[J_y^p(i, j) + J_y^p(i, j + 1)], \\ J_z(i, j) &\equiv J_z^p(i, j). \end{aligned} \quad (8)$$

The six field components, E_x , E_y , E_z , B_x , B_y , and B_z are then all integrated exactly as prescribed by the staggered-leapfrog algorithm. These field components

are, however, averaged back to the particle grid before being used to advance the particle equations of motion. Thus,

$$\begin{aligned}
 E_x^p(i, j) &\equiv 1/2[E_x(i + 1/2, j) + E_x(i - 1/2, j)], \\
 E_y^p(i, j) &\equiv 1/2[E_y(i, j + 1/2) + E_y(i, j - 1/2)], \\
 E_z^p(i, j) &\equiv E_z(i, j), \\
 B_x^p(i, j) &\equiv 1/2[B_x(i, j + 1/2) + B_x(i, j - 1/2)], \\
 B_y^p(i, j) &\equiv 1/2[B_y(i + 1/2, j) + B_y(i - 1/2, j)], \\
 B_z^p(i, j) &\equiv 1/4[B_z(i + 1/2, j + 1/2) + B_z(i + 1/2, j - 1/2) \\
 &\quad + B_z(i - 1/2, j + 1/2) + B_z(i - 1/2, j - 1/2)].
 \end{aligned} \tag{9}$$

The original fields \mathbf{E} and \mathbf{B} are retained unchanged, however, for use in the next cycle to advance Maxwell's equations. They are *not* to be computed as averages of the particle fields \mathbf{E}^p and \mathbf{B}^p .

The averaging at a boundary is straight forward. One uses the value of the field in the cell just across the boundary. This value is, of course, determined by the type of boundary condition specified. For example, for a perfect conductor where the perpendicular component of the electric field is specified on a point one half cell from the wall, the value of the field on the image cell one half grid space into the wall is the same and the averaging is preformed exactly as specified previously.

The immediate consequence of adding the averaging stages given by Eqs. (8) and (9) to standard fully electromagnetic codes is the removal of nonphysical electrostatic and magnetostatic self forces. There are two other favorable and important consequences. First, the averages required are smoothing operations; therefore, spurious numerical Cherenkov radiation and *bremmstrahlung*, arising mostly at short wavelengths, will be partially suppressed. Second, a sizable simplification results since all particle quantities are now defined on a single grid. Only one set of bilinear weight coefficients need be found, rather than four, and, thus, it is expected that optimized particle integration can be speeded up by at least a factor of two.

REFERENCES

1. J. P. BORIS, "Proceedings of the Fourth Conference on Numerical Simulation of Plasmas," pp. 3-67, National Research Laboratory, Washington, D. C., November 2-3, 1970.
2. J. P. BORIS AND R. LEE, "Computations on Relativistic Electron Beams and Rings," Proceedings, Eleventh Symposium on Electron, Ion, and Laser Beam Technology, Boulder, Colorado, May 1971.
3. O. BUNEMAN, "Fast Numerical Procedures for Computer Experiments on Relativistic Plasmas," in "Relativistic Plasmas — The Coral Gables Conference" (O. Buneman and W. Pardo, Eds.), University of Miami, 1968, W. A. Benjamin, New York, 1968.

4. A. B. LANGDON AND J. M. DAWSON, "Investigations of A. Sheet Model for a Bounded Plasma with Magnetic Field and Radiation," Memorandum ERL-M-257, Electronics Research Laboratory, University of California, Berkeley, CA, January 1969.
5. K. H. SINZ, "Proceedings of the Fourth Conference on Numerical Simulations of Plasmas," pp. 153-164, National Research Laboratory, Washington, D. C., November 2-3, 1970.
6. R. L. MORSE AND C. W. NIELSON, *Phys. Fluids* **14** (1971), 830.
7. A. B. LANGDON, *Phys. Fluids* **15** (1972), 1149.
8. C. K. BIRDSALL AND D. FUSS, *J. Computational Phys.* **3** (1969), 494-511.
9. R. L. MORSE AND C. W. NIELSON, *Phys. Fluids* **12** (1969), 2418.
10. A. B. LANGDON AND C. K. BIRDSALL, private communications.

RECEIVED: March 17, 1972

JAY P. BORIS
ROSWELL LEE

*Naval Research Laboratory
Washington, D. C. 20375*